



# Cellobiose Consumption Uncouples Extracellular Glucose Sensing and Glucose Metabolism in *Saccharomyces cerevisiae*

Kulika Chomvong,<sup>a</sup> Daniel I. Benjamin,<sup>b</sup> Daniel K. Nomura,<sup>b</sup> Jamie H. D. Cate<sup>c,d,e</sup>

Department of Plant and Microbial Biology, University of California, Berkeley, California, USA<sup>a</sup>; Department of Nutritional Sciences and Toxicology, University of California, Berkeley, California, USA<sup>b</sup>; Department of Molecular and Cell Biology, University of California, Berkeley, California, USA<sup>c</sup>; Department of Chemistry, University of California, Berkeley, California, USA<sup>d</sup>; Molecular Biophysics and Integrated Bioimaging Division, Lawrence Berkeley National Laboratory, Berkeley, California, USA<sup>e</sup>

**ABSTRACT** Glycolysis is central to energy metabolism in most organisms and is highly regulated to enable optimal growth. In the yeast *Saccharomyces cerevisiae*, feedback mechanisms that control flux through glycolysis span transcriptional control to metabolite levels in the cell. Using a cellobiose consumption pathway, we decoupled glucose sensing from carbon utilization, revealing new modular layers of control that induce ATP consumption to drive rapid carbon fermentation. Alterations of the beta subunit of phosphofructokinase-1 (*PFK2*), H<sup>+</sup>-plasma membrane ATPase (*PMA1*), and glucose sensors (*SNF3* and *RGT2*) revealed the importance of coupling extracellular glucose sensing to manage ATP levels in the cell. Controlling the upper bound of cellular ATP levels may be a general mechanism used to regulate energy levels in cells, via a regulatory network that can be uncoupled from ATP concentrations under perceived starvation conditions.

**IMPORTANCE** Living cells are fine-tuned through evolution to thrive in their native environments. Genome alterations to create organisms for specific biotechnological applications may result in unexpected and undesired phenotypes. We used a minimal synthetic biological system in the yeast *Saccharomyces cerevisiae* as a platform to reveal novel connections between carbon sensing, starvation conditions, and energy homeostasis.

**KEYWORDS** PMA1, cellobiose, glucose sensors, metabolomics

Most microorganisms favor glucose as their primary carbon source, as reflected in their genetic programs hard-wired for this preference. Central to carbon metabolism is glycolysis, which is finely tuned to the dynamic state of the cell due to the fact that glycolysis first consumes ATP before generating additional ATP equivalents. To avoid catastrophic depletion of ATP, the yeast *Saccharomyces cerevisiae* has evolved a transient ATP hydrolysis futile cycle coupled to gluconeogenesis (1). Glycolysis in yeast is also tightly coupled to glucose transport into the cell, entailing three extracellular glucose-sensing mechanisms and at least one intracellular glucose signaling pathway (2).

Synthetic biology and metabolic engineering of yeast hold promise to convert this microorganism into a “cell factory” to produce a wide range of chemicals derived from renewable resources or those unattainable through traditional chemical routes. However, many applications require tapping into metabolites involved in central carbon metabolism, a daunting challenge as living cells have numerous layers of feedback regulation that fine-tune growth to changing environments. Cellular regulation evolved

Received 22 May 2017 Accepted 3 July 2017 Published 8 August 2017

**Citation** Chomvong K, Benjamin DI, Nomura DK, Cate JHD. 2017. Cellobiose consumption uncouples extracellular glucose sensing and glucose metabolism in *Saccharomyces cerevisiae*. mBio 8:e00855-17. <https://doi.org/10.1128/mBio.00855-17>.

**Editor** Jizhong Zhou, University of Oklahoma

**Copyright** © 2017 Chomvong et al. This is an open-access article distributed under the terms of the [Creative Commons Attribution 4.0 International license](https://creativecommons.org/licenses/by/4.0/).

Address correspondence to Jamie H. D. Cate, [jcate@lbl.gov](mailto:jcate@lbl.gov).

intricate networks to maintain and ensure cell survival. For example, *S. cerevisiae* has evolved to rapidly consume high concentrations of glucose through fermentation while repressing the expression of other carbon consumption pathways, an effect termed glucose repression. When perturbed genetically, regulatory networks such as those in glucose repression often generate undesirable or unexpected phenotypes.

For yeast to be useful in producing large volumes of renewable chemicals or biofuels, it will be important to expand its carbon utilization to include multiple sugars in the plant cell wall. One promising approach that helps overcome glucose repression and allows simultaneous utilization of different sugars is cellobiose consumption (3). Cellobiose is a disaccharide with two units of glucose linked by a  $\beta$ -1,4 glycosidic bond. Cellobiose consumption using a minimal additional pathway in yeast—a cellodextrin transporter (CDT-1) and intracellular  $\beta$ -glucosidase (4)—avoids glucose repression by importing carbon in the form of cellobiose instead of glucose. The cellodextrin transporter allows cellobiose to enter the cell, where it is hydrolyzed to glucose and consumed via the native glycolytic consumption pathway. By moving glucose production into the cell, the *Neurospora crassa*-derived cellobiose consumption pathway is nearly the minimal synthetic biological module imaginable in *S. cerevisiae*, comprised of just two genes. Nevertheless, in *S. cerevisiae* the cellobiose consumption pathway is inferior to consumption of extracellular glucose in terms of rate and results in a prolonged lag phase (5). Previous efforts to understand the impact of cellobiose consumption on the physiology of *S. cerevisiae* using transcriptional profiling revealed that cellobiose improperly regulates mitochondrial activity and amino acid biosynthesis, both of which are tightly coupled to the transition from respiration to fermentation (5).

Since glycolytic enzymes are regulated mostly at the posttranscriptional level (6), we probed cellobiose consumption in *S. cerevisiae* at the metabolite level. We found that key metabolites in glycolysis are highly imbalanced, leading to low flux through glycolysis and slow fermentation. We also found that excess ATP levels drive the imbalance and identified a new potential regulatory role of glucose sensors in cellular ATP homeostasis.

## RESULTS

**Metabolite profiling of cellobiose utilizing *S. cerevisiae*.** *S. cerevisiae* cells engineered with the cellobiose consumption pathway exhibit a prolonged lag phase, with decreased growth and carbon consumption rates in comparison to those when glucose is provided (see Fig. S1A in the supplemental material) (5). We hypothesized that cellobiose consumption results in an ATP deficit in glycolysis relative to glucose, due to the fact that the cellodextrin transporter (CDT-1) in the cellobiose-utilizing pathway is a proton symporter, requiring ATP hydrolysis for cellobiose uptake (7). Moreover, under anaerobic conditions, ATP production is limited to substrate-level phosphorylation, further restricting ATP availability. We measured the steady-state concentrations of ATP and other metabolites in central carbon metabolism in yeast fermenting cellobiose compared to those fermenting glucose. Of the 48 compounds analyzed, the abundance of 25 compounds was significantly different between cellobiose- and glucose-fed samples (Fig. S1B). Surprisingly, ATP levels increased by 6-fold in the cellobiose-grown cells (Fig. 1A). The relative abundance of compounds in glycolysis—fructose 6-phosphate (F6P), glucose 6-phosphate (G6P), glucose, and pyruvate—increased by 444-, 81-, 7-, and 3-fold, respectively, while that of phosphoenolpyruvate (PEP) decreased by 2-fold (Fig. 1A and B). These results suggest that the yeast cells underwent drastic physiological changes, reflected in metabolite levels, when cellobiose was provided in place of glucose.

**Phosphofructokinase-1 inhibition by excess ATP.** Given the dramatic buildup of glucose, G6P, and F6P intermediates prior to the phosphofructokinase-1 (Pfk1) reaction in glycolysis (Fig. 1B and 2A), we reasoned that Pfk1 might be a major bottleneck in cellobiose consumption. Pfk1 catalyzes the phosphorylation of F6P, using one ATP and yielding fructose 1,6-bisphosphate (F1,6BP) as a product. As the second committed step in glycolysis, Pfk1 is heavily regulated—with ATP acting as an allosteric inhibitor and AMP and fructose 2,6-bisphosphate (F2,6BP) serving as activators (8–10).

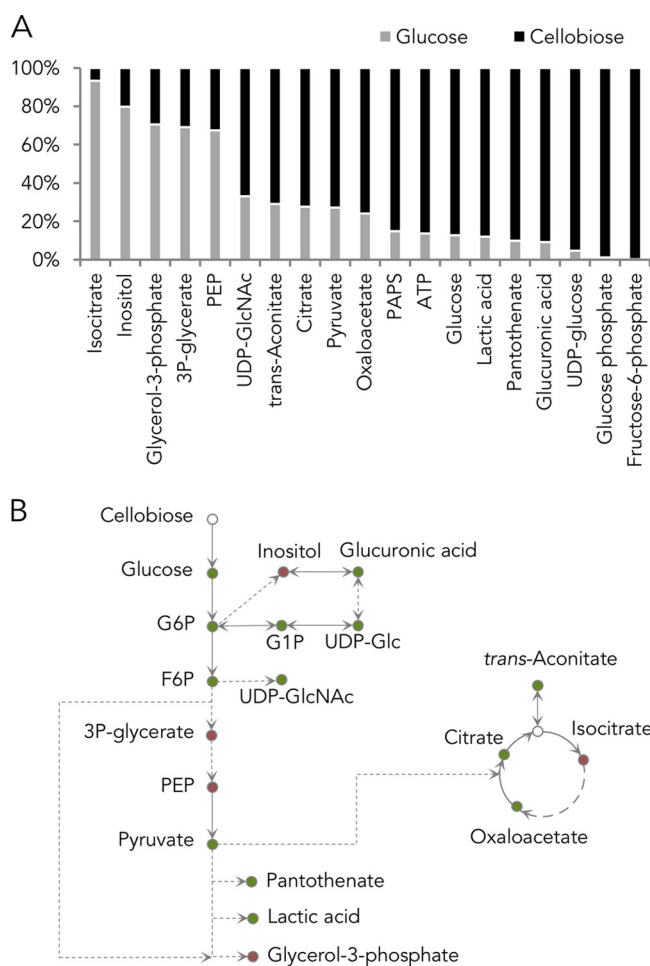


**FIG 1** Metabolite profile of cells provided with glucose or cellobiose. (A) Significant changes of intracellular metabolite levels in cells provided with cellobiose compared to cells provided with glucose as a sole carbon source. (B) Schematic representation of metabolite changes. Relative metabolite level: higher in cellobiose condition (green) and higher in glucose condition (red). Statistical analyses are described in Materials and Methods.

To test whether allosteric inhibition of Pfk1 by ATP limited cellobiose fermentation, a mutation in Pfk1 that makes the enzyme ATP insensitive (P722L in the Pfk1 beta subunit; note that the original publication referred to this mutation as P728L [11]) was introduced into the chromosomally carried *PFK2* gene (mutation here termed *pfk1m*) in the cellobiose-utilizing strain. This mutation was previously shown to reduce not only ATP inhibition but also AMP and fructose 2,6-bisphosphate activation of Pfk1 in *S. cerevisiae* (11). We chose this mutation over an ATP-insensitive, AMP/F2,6BP-sensitive mutant phosphofructokinase (10) because the latter's phenotype has not been evaluated in *S. cerevisiae*. High initial cell densities were used thereafter, as the focus of this study is sugar consumption rather than growth.

Consistent with allosteric inhibition of Pfk1 by ATP, the cellobiose consumption efficiency ( $E_c$ ) of the *pfk1m* strain increased by 33% in comparison to the strain with wild-type (WT) Pfk1 (Fig. 2B). In these high cell densities, negligible changes in growth rate were observed (Fig. 2C). The relative abundance of G6P and F1,6BP decreased by 47% and 34%, respectively, while that of ATP remained relatively unchanged (Fig. 2D). The unchanged ATP level was expected as the ATP requirement for the cellobiose consumption pathway was likely offset by the ATP generated as part of carbon metabolism. These results indicate that the 6-fold increase in cellular ATP concentrations allosterically inhibited Pfk1, resulting in accumulation of glucose, G6P, and F6P, which eventually slowed down cellobiose consumption.

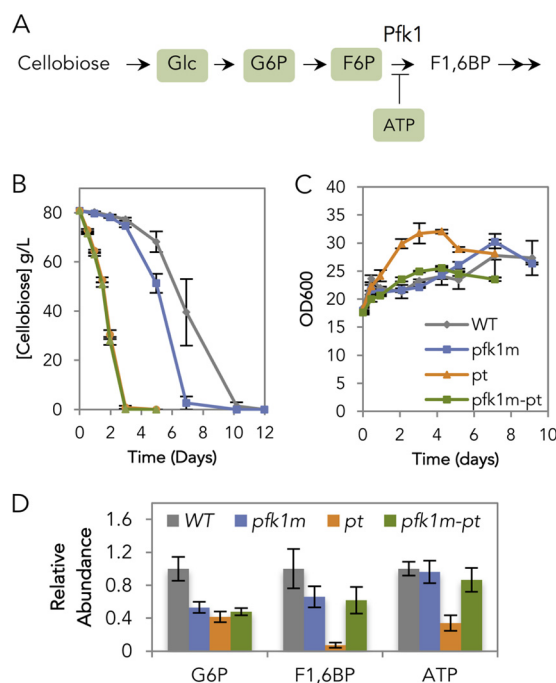


**FIG 2** Manipulation of phosphofructokinase-1 (*PFK2*) and plasma membrane ATPase (*PMA1*). (A) Schematic representation of cellobiose consumption route in the upper glycolytic pathway. Glc, G6P, F6P, and ATP are highlighted and were found in higher abundance when cellobiose was provided than when glucose was provided. (B and C) Cellobiose consumption profile (B) and cell density profile (C) of the strains with ATP-insensitive Pfk1 (*pfk1m*), constitutively active Pma1 (*pt*), and the combination of the two mutations (*pfk1m-pt*) in comparison to the cellobiose pathway-only strain, here used as the wild type (WT). (D) Relative abundance of G6P, F1,6BP, and ATP levels of the WT, *pfk1m*, *pt*, and *pfk1m-pt* strains, relative to the WT strain fermenting cellobiose. The experiments were carried out in five biological replicates, with standard errors of the means shown.

**Limited activity of plasma membrane ATPase.** Although the *pfk1m* strain partially increased the rate of cellobiose fermentation, cellular ATP remained elevated relative to glucose fermentation. It is unlikely that ATP production was the cause of the difference, as fermentation is limited to substrate-level phosphorylation under anaerobic conditions regardless of carbon source. We therefore tested whether the activity of one of the major ATP sinks in yeast, the plasma membrane ATPase (*Pma1*), was responsible for the ATP buildup. *Pma1* hydrolyzes 25 to 40% of cellular ATP in yeast (12) and is heavily regulated by glucose (13).

A constitutively active mutant form of *PMA1* (*pma1-Δ916*, here abbreviated *pt*) (14) was introduced into the endogenous *PMA1* locus in the cellobiose-utilizing strain. This mutation results in high *Pma1* ATPase activity even under carbon starvation conditions (14). The  $E_c$  of the *pt* strain was four times that of the control (Fig. 2B), whereas the growth rate of the *pt* strain was only slightly higher than that of the *Pma1* wild-type (WT) strain (Fig. 2C). As expected, we observed a 66% decrease in cellular ATP levels in the *pt* strain in comparison to the WT control (i.e., cellobiose pathway only) (Fig. 2D). In addition, the concentrations of G6P and F1,6BP decreased by 58% and 93%, respectively, relative to strains expressing wild-type *PMA1*. Notably, these concentrations dropped more than when the ATP-insensitive Pfk1 mutant was introduced (Fig. 2D). These results suggest that increased *Pma1* ATPase activity improved cellobiose fermentation. We hypothesize that the drastic decrease in F1,6BP level and the high growth rate were the result of rapid glycolytic flux, as the cells experience low cellular ATP levels in the *pt* strain.

Next, we observed the phenotypes of the *pfk1m-pt* double mutant strain. The cellobiose consumption profile of a *pfk1m-pt* double mutant was identical to that of the *pt* strain (Fig. 2A). However, the growth rate and relative abundance of G6P, F1,6BP, and

ATP of the *pfk1m-pt* strain differed from those of the *pt* strain (Fig. 2C and D). In fact, their levels were similar to those in the *pfk1m* strain. These results imply that while the ATP might be hydrolyzed rapidly due to the *pt* effect, the removal of ATP inhibition of *pfk1* allowed enough ATP to be regenerated downstream that no drastic decrease in ATP was observed. The underlying explanation of the mixed phenotypes will require future experiments to dissect how Pfk1 exerts allosteric control on glycolysis and ATP levels.

**Carbon starvation-like state of the plasma membrane ATPase.** Although cellobiose theoretically provides the same energy and carbon availability to cells as glucose, it releases glucose only after intracellular hydrolysis by  $\beta$ -glucosidase. Thus, the cellobiose consumption system used here does not generate extracellular glucose, which acts as a crucial signaling molecule for yeast carbon metabolism. Taken together with the observation that increased ATPase activity in the *pt* strain increased cellobiose consumption efficiency, we wondered whether the limited Pma1 activity in cellobiose-fed cells is due to the absence of extracellular glucose in the medium. Transcriptionally, the presence of glucose increases *PMA1* mRNA levels by 2 to 4 times via the regulation of Rap1, Gcr1, and Sir2 (15–17). Consistent with the requirement for extracellular glucose sensing, previous RNA sequencing experiments revealed a 40% decrease in *PMA1* transcript levels when cellobiose was provided in place of glucose (5). However, although transcriptional regulation of *PMA1* is important, it is slower than posttranscriptional regulation and results in smaller changes (13, 18).

In the presence of glucose, phosphorylation of Ser-899 decreases Pma1's  $K_m$  and Ser-911/Thr-912 increases Pma1's  $V_{max}$  for ATP, respectively (13, 19, 20). Given the 6-fold excess amount of ATP observed under cellobiose-utilizing conditions (Fig. 1A), the effective velocity of the Pma1 reaction is likely approaching  $V_{max}$  regardless of the phosphorylation status at Ser-899 (21). The  $K_m$  of ATP hydrolysis by Pma1 has been reported to increase approximately 3-fold from 1.2 mM in glucose-fermenting cells to 4.0 mM in glucose-starved cells, while a 10-fold decrease in  $V_{max}$  was reported in the same study (22). We reasoned that the 6-fold increase of ATP in cellobiose-fed cells should result in ATP concentrations in excess of the  $K_m$  for Pma1, resulting in Pma1 activity being limited by its  $V_{max}$ . Thus, in this study, we did not investigate the phosphorylation of Ser-899 and chose to investigate whether  $V_{max}$ -determining phosphorylation states of Ser-911 and Thr-912 might play a major role in establishing the efficiency of cellobiose fermentation (Fig. 3A).

Combinatorial mutations of Ser-911/Thr-912 to alanine and aspartic acid were introduced into the endogenous *PMA1* gene to prevent or mimic phosphorylation, respectively. We were unable to obtain strains with *pma1-S911A/T912A* and *pma1-S911A/T912D*, potentially because the combinations were lethal. All mutant strains whose Pma1 S911 position was mutated to aspartic acid consumed cellobiose more efficiently than when the S911 position remained unchanged (Fig. 3B). In contrast, mutating Pma1 T912 to aspartic acid did not show a correlation with the cellobiose consumption phenotype. These results suggest that phosphorylation of Pma1 at S911 was lacking when cellobiose was provided as a sole carbon source.

**Positive effects of extracellular glucose sensor deletions.** According to the above mutational analysis, the Pma1 phosphorylation state of cellobiose-fed cells was similar to that under carbon starvation conditions (Fig. 3A) (20). In the previously published experiments (20), carbon-starved cells were prepared by incubating mid-exponential-phase cells in medium without glucose. Under such conditions, neither extracellular nor intracellular glucose is present. For the cellobiose-fed cells, based on the relatively high level of intracellular glucose that we detected (Fig. 1A), it is unlikely that the intracellular glucose induced Pma1 carbon starvation. Additionally, since intracellular glucose metabolism is expected in cellobiose-fed cells, its effect on Pma1 carbon starvation was also ruled out (23). We therefore tested the role of extracellular glucose in regulating Pma1 activity. In cellobiose-fed cells, glucose is not provided as part of the medium,

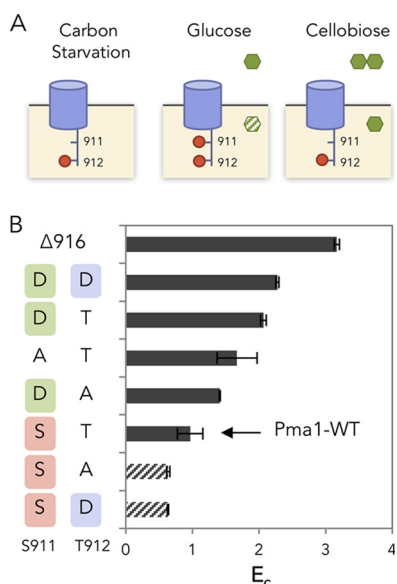


**FIG 3** Carbon starvation-like state of the plasma membrane ATPase (*PMA1*) in cellobiose-fermenting cells. (A) Phosphorylation states of Pma1 residues S911 and T912 under carbon starvation, glucose-metabolizing, and cellobiose-metabolizing conditions. (B) Cellobiose consumption efficiency ( $E_c$ ) of cells expressing Pma1 with phospho-mimic or phosphorylation-preventing mutations at positions serine 911 (S911) and threonine 912 (T912). Phospho-mimic and phosphorylation-preventing mutations at position S911 are presented in green and red, respectively. Phospho-mimic mutations at position T912 are presented in blue. Shown are the means and standard deviations for three biological replicates. The experiments were carried out in two biological replicates, with standard errors of the means shown.

and thus, the extracellular glucose is absent. We hypothesize that the extracellular glucose is likely essential for full activation of Pma1 through S911 phosphorylation.

*Snf3*, *Rgt2*, and *Gpr1* are the three known sensors of extracellular glucose in *S. cerevisiae*. *Snf3* and *Rgt2* mainly regulate glucose transport while *Gpr1* controls cell physiology via an interaction with *Gpa2* to activate protein kinase A and cyclic AMP (cAMP) synthesis (23). To mimic the presence of extracellular glucose, constitutively active mutations (*snf3* R229K, *rgt2* R231K, and *gpa2* R273A) were introduced into the endogenous loci to probe the role of each glucose-sensing pathway (24, 25). Surprisingly, the cellobiose consumption efficiency of all three mutant strains decreased by ~25% (Fig. S2A). We then inverted the genetic modifications by deleting *SNF3*, *RGT2*, and/or *GPA2*. Notably, the triple glucose-sensing deletion strain (*snf3* $\Delta$  *rgt2* $\Delta$  *gpa2* $\Delta$  [abbreviated *srg* $\Delta$ ]) showed a 275% increase in  $E_c$  (Fig. 4A).

Combinatorial deletions revealed that the *Gpr1* pathway did not contribute to improved cellobiose fermentation, but combining the *SNF3* and *RGT2* deletions (*sr* $\Delta$ ) was necessary and sufficient to replicate the  $E_c$  of the triple deletion strain (Fig. 4A and S2B and C). Consistent with the observed  $E_c$  values, the intracellular ATP levels of *srg* $\Delta$  and *sr* $\Delta$  decreased by 41% and 18%, respectively, while those in the individual-deletion *snf3* $\Delta$  and *rgt2* $\Delta$  strains remained unchanged (Fig. 4A). These results reveal a negative correlation between  $E_c$  and cellular ATP levels (Fig. 4B) and showed that *Snf3* and *Rgt2* acted together to regulate cellular ATP levels, in addition to regulating glucose transport.

Although the additional deletion of *GPA2* (*gpa2* $\Delta$ ) in the *sr* $\Delta$  strain did not further improve  $E_c$  (Fig. 4A), it reduced the relative abundance of ATP by 28%, implying that the *Gpr1* pathway has a separate mechanism to control cellular ATP levels that does not directly affect carbon metabolism. Consistently, *gpa2* $\Delta$  had a negative or neutral impact on cellobiose consumption (Fig. S2). The decrease in ATP level may be a result of altered cellular activities, controlled by *Gpr1* via the Tor and cAMP-protein kinase A (PKA)-Ras pathways (23). The relationship between *Gpr1*-regulated ATP levels and carbon metabolism remains to be discovered. Since *gpa2* $\Delta$  did not have a direct effect on  $E_c$ , it was not investigated further in this study.

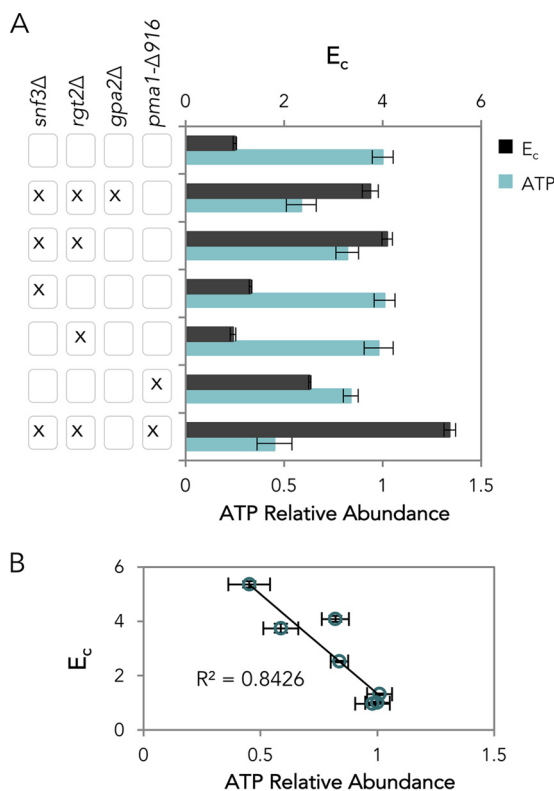


**FIG 4** Effect of glucose sensor deletions. (A) Cellobiose consumption efficiency ( $E_c$ ) and cellular ATP levels of strains with different glucose sensor deletions and different combinations of constitutively active Pma1 mutations. Shown are the averages and standard deviations of three biological replicates. (B) Correlation of  $E_c$  and cellular ATP. Standard deviations for three biological replicates are shown for each point.

**Snf3/Rgt2 regulation of cellular ATP levels.** To examine whether Snf3/Rgt2 regulated the cellular ATP level in cellobiose fermentations via Pma1, an *snf3Δ rgt2Δ pma1-Δ916* strain (*srΔ-pt* strain) was constructed. Notably, the  $E_c$  of the *srΔ-pt* strain increased more than four times in comparison to the wild-type control (Fig. 4A and 5A). The improvement was additive, within the range of the  $\Delta E_c$  summation of the *srΔ* and *pma1-Δ916* strains relative to the wild type (Fig. 5A). Although ATP levels decreased in a nearly linear fashion as a function of  $E_c$  (Fig. 4B), it is not currently possible to ascertain whether the *srΔ* and *pma1-Δ916* mutations act entirely independently due to limitations in measurement accuracy (Fig. 5A).

To further determine the relationship between Snf3/Rgt2 and Pma1, the vanadate-specific ATPase activity of Pma1 (26) from different strains consuming cellobiose was analyzed (Fig. 5B). Consistent with the constitutively active nature of the *pt* mutation, the activities of Pma1 in the *pt* and *srΔ-pt* strains were higher than those observed in the WT or *srΔ* strain, respectively. Addition of *srΔ* decreased the Pma1 ATPase activities by 25% and 32% in WT and *pt* strains, respectively. In other words, the absence of Snf3 and Rgt2 led to a partial decrease in Pma1 ATPase activity, which implied that Snf3/Rgt2 partially activated Pma1 ATPase activity in the absence of glucose.

## DISCUSSION

To identify the effects of a minimal alteration to carbon metabolism in yeast, we chose a cellobiose-consumption pathway composed of two genes and analyzed its cellular metabolite profiles in comparison with cells provided with glucose, yeast's preferred carbon source (Fig. 6). Here, we focus on the cellobiose consumption efficiency ( $E_c$ ), as  $E_c$  linearly correlated with ethanol production rate, while ethanol yield remained mostly unchanged (see Fig. S3 in the supplemental material).

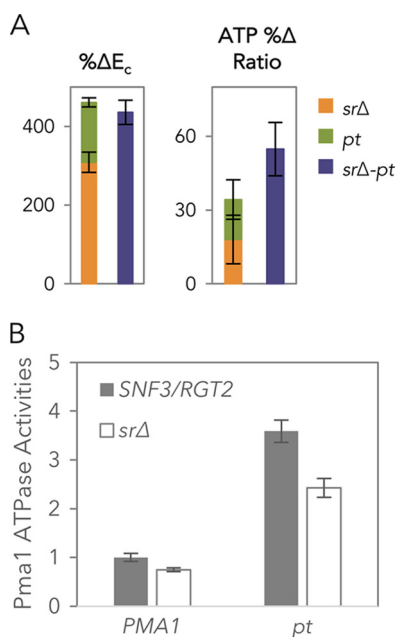


**FIG 5** Glucose sensor deletions and cellular ATP levels. (A) Additive effect of the increase in  $E_c$  and the decrease in cellular ATP of *srΔ* and *pt* in the *srΔ-pt* strain. The experiments were carried out in five biological replicates, with standard errors of the means shown. (B) Specific Pma1 ATPase of WT, *pt*, *srΔ*, and *srΔ-pt* strains measured from normalized membrane fractions of cells harvested at mid-log phase. The experiments were carried out in three biological replicates, with standard errors of the means shown.

More than half of the metabolites significantly changed in abundance when cellobiose was provided in place of glucose. The buildup of G6P, F6P, and ATP in *S. cerevisiae* fermenting cellobiose suggested that Pfk1 was one of the bottlenecks in the process. Pfk1 is subjected to complex allosteric regulation, including inhibition by ATP and

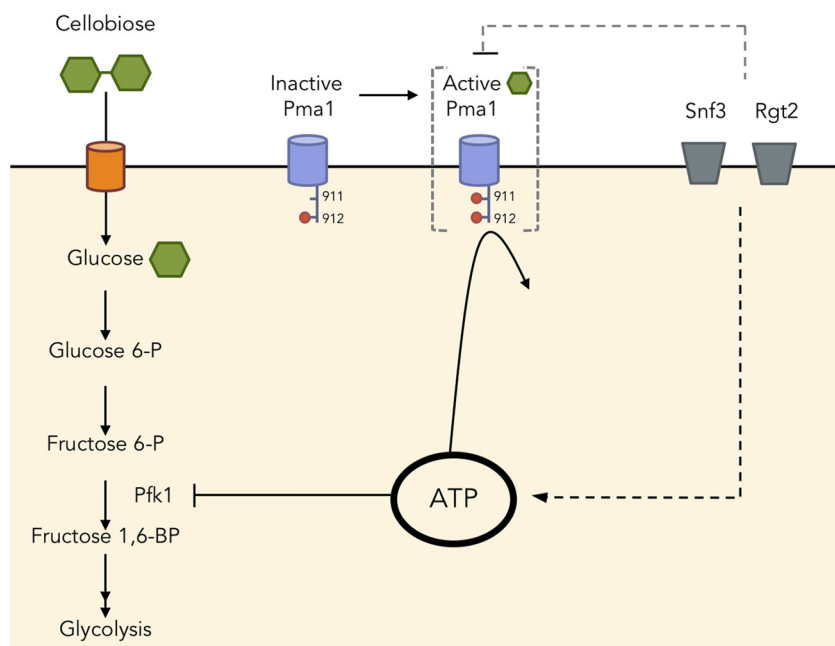


**FIG 6** Schematic representation of ATP homeostasis and cellular regulation of cellobiose fermentation. Excess ATP inhibited phosphofructokinase (Pfk1), resulting in an upper glycolytic metabolite buildup and slow cellobiose consumption. The buildup of ATP may be caused by low activity of Pma1, with no phosphorylation at position 911. Additionally, glucose sensors Snf3 and Rgt2 together influenced cellular ATP levels via Pma1 and other mechanisms yet to be identified.

activation by AMP and fructose 2,6-bisphosphate (F2,6BP) (8–10). The Pfk1 bottleneck was partially relieved in cells expressing an ATP/AMP/F2,6BP-insensitive *PFK2* allele, while the ATP level remained elevated. These results contrast with previous studies that identified ATP depletion and the buildup of fructose 1,6-bisphosphate—the metabolite immediately downstream of Pfk1—as a weak link in glycolysis (1). Although we did not investigate the effect of AMP and F2,6BP activation since their changes between glucose and cellobiose conditions were less than 2-fold and they did not meet the significance threshold of a *P* value less than 0.01, it is possible that they could influence cellobiose consumption efficiency.

ATP is central to a cell's energy currency, but too much ATP is not necessarily beneficial (27, 28). In fact, we observed a negative correlation between cellular ATP levels and cellobiose consumption efficiency (Fig. 4B). A similar correlation has been reported for glucose as a carbon source, suggesting metabolic uncoupling of energy homeostasis in yeast cells (29). We propose that intracellular glucose concentrations—generated by cellobiose hydrolysis in our experiments—and glucose metabolism (23) are insufficient to trigger glucose activation of key metabolic pathways and enzyme activity. For example, we found that the ATP-dependent proton pump Pma1 existed in a carbon-starvation-like state during cellobiose fermentation and was partially responsible for the aberrant accumulation of ATP. These results suggest that neither intracellular glucose nor glucose metabolism is sufficient to fully activate Pma1. A previous study showed the lack of phosphorylation of S899 and S911/T912 in Pma1, in a hexokinase/glucokinase deletion strain (*hxxk1Δ hxxk2Δ glk1Δ*) provided with glucose, suggesting that phosphorylation of these residues requires glucose metabolism (30). Together with our results, we propose that the activation of Pma1 through S911 phosphorylation requires both extracellular glucose and glucose metabolism. Our results reveal that the cellobiose utilization system allows uncoupling of glucose metabolism and intracellular glucose from extracellular glucose signaling. Future experiments will be required to reveal why ATP was not consumed by other cellular processes triggered under starvation (31).

Cytosolic pH is also a key regulator of carbon utilization (32) and is likely to be impacted by the use of the proton symporter CDT-1 for cellobiose import and the resulting low activity of Pma1. High cytosolic pH is necessary and sufficient to activate Tor-Ras-PKA activities, which are downstream of the Gpr1 glucose-sensing pathway (32). In contrast, the proton symporter CDT-1 and low activity of Pma1 may result in a low cytosolic pH. However, cytosolic pH alone is unlikely to determine the cellobiose consumption efficiency ( $E_c$ ), as the strain with an ATP/AMP/F2,6BP-insensitive *PFK2* allele showed improved  $E_c$  but unaltered cellular ATP levels. Furthermore, the inactivation of the Gpr1 pathway resulted in decreased cellular ATP but unaltered  $E_c$ . Glucose storage, i.e., in the form of trehalose, may be interconnected through the Gpr1 pathway because Ras-cAMP activates trehalase, required to break down trehalose—a phenomenon observed when gluconeogenesis is switched to glycolysis (33). Trehalose cycling has been shown to lead to an imbalanced state of glycolysis (1). The relationship between carbon storage and  $E_c$  will require future studies to examine this relationship.

We also found that the well-studied extracellular glucose sensors Snf3 and Rgt2 exhibited a novel role in cellular ATP homeostasis partially through the major plasma membrane ATPase Pma1. Deletion of extracellular glucose sensors (Snf3 and Rgt2) increased cellobiose consumption efficiency and partially restored ATP levels. Interestingly, the absence of Snf3/Rgt2 decreased Pma1 ATPase activities, an effect that should have led to an increase in ATP level. The restored low ATP level observed in the *srΔ* strain implied that Snf3/Rgt2 regulated cellular ATP level with an additional mechanism(s) other than that through Pma1. It is known that deletion of *SNF3* and *RGT2* slows down glucose consumption (34), due to the inability of these strains to degrade Mth1 and Std1, which block the promoter regions of hexose transporters required for optimal glucose import (35–38). Unlike glucose, cellobiose does not signal Mth1 degradation even with intact Snf3/Rgt2 (38). Thus, genes downstream of Mth1 regulation, including hexose transporters, are not expected to be responsible for the improved  $E_c$  and

decreased cellular ATP levels observed in the *srΔ* strain. Consistent with this model, no growth defect is observed in an *mth1Δ* strain growing on glucose, suggesting that Snf3/Rgt2 has additional regulatory nodes other than Mth1 (34). Future transcriptional profiling and ribosome profiling experiments will be required to reveal the additional Snf3/Rgt2 roles in cellular ATP homeostasis.

The present systems-level study of a minimal synthetic biology pathway for cellobiose consumption revealed the dramatic impact of decoupling extracellular and intracellular glucose sensing, resulting in an overabundance of ATP in cells. The inability of *S. cerevisiae* to catabolize ATP for cellular processes in the presence of intracellular glucose and glucose metabolism but in the absence of extracellular glucose resulted in slow fermentation. Thus, ATP levels must be kept in a relatively narrow range for optimal fermentation and to allow robust startup of glycolysis, and yet yeast seems to lack a direct mechanism to monitor ATP concentrations. For example, a dynamic model showed that a small concentration difference of inorganic phosphate, a product of ATP hydrolysis, could alter cell fate from a stable glycolytic steady state to an imbalanced dead-end state (1). Here, we found that the extracellular glucose sensing by Snf3/Rgt2 required for optimal glucose fermentation (2) can be uncoupled from the role of these receptors in regulating ATP homeostasis under carbon starvation conditions. It will be important in the future to map the full regulatory pathways of ATP homeostasis leading from Snf3/Rgt2 and, independently, terminating in Pma1.

## MATERIALS AND METHODS

**Yeast strains, media, and anaerobic fermentation.** The *S. cerevisiae* background strain used in this study was S288C *ura3::P<sub>PGK1</sub>-cdt-1* N209S/F262Y-*T<sub>ADH1</sub>* *lyp1::P<sub>TDH3</sub>-gh1-1* (codon optimized)-*T<sub>CYC1</sub>* derived by chromosomal DNA library selection (39). The strain was subjected to further modifications using the CRISPRm system (39). The list of strains constructed, CRISPRm guides, and primers used are included in Table S1 in the supplemental material.

Seed cultures for cellobiose fermentation experiments were grown in optimal minimal medium (oMM) (5) with 20 g/liter of glucose and harvested at mid-log phase. All cellobiose fermentation experiments were conducted under strict anaerobic conditions, in oMM with 80 g/liter of cellobiose at an initial optical density at 600 nm ( $OD_{600}$ ) of 20, using 10-ml serum flasks containing 5 ml fermentation mixture in 2 to 5 biological replicates. The flasks were incubated at 30°C and 220 rpm. The cellobiose consumption efficiency ( $E_c$ ) was defined as the inverse of the area under the curve of extracellular cellobiose concentration over time.

**Analytical analysis of yeast metabolites.** Extracellular cellobiose concentrations were determined by high-performance liquid chromatography (HPLC) on a Prominence HPLC (Shimadzu, Kyoto, Japan) equipped with a Rezex RFX-FastAcid H 10- by 7.8-mm column. The column was eluted with 0.01 N of  $H_2SO_4$  at a flow rate of 1 ml/min at 55°C.

For the metabolite profiling comparison between glucose and cellobiose (modified from reference 40), equal amounts of yeast cells at mid-exponential phase of anaerobic sugar consumption (10 g/liter cellobiose or glucose) were harvested (final pellet  $OD_{600}$  equivalent to 5). The samples were quenched in 180  $\mu$ l of 40:40:20 acetonitrile-methanol-water. Following the addition of 10 nmol of d3 serine (as an internal standard), the mixtures were vortexed and centrifuged at 13,000 rpm for 10 min. The supernatants were injected onto an Agilent 6460 QQQ liquid chromatography-tandem mass spectrometer (LC-MS/MS), and the chromatography was achieved by normal phase separation with a Luna  $NH_2$  column (Phenomenex) starting with 100% acetonitrile with a gradient to 100% 95:5 water-acetonitrile. Formic acid (0.1%) or 0.2% ammonium hydroxide with 50 mM ammonium acetate was added to assist with ionization in positive and negative ionization mode, respectively. Five biological replicates were used for each sample analyzed.

For targeted intracellular metabolite comparisons, yeast cells equivalent to 20  $OD_{600}$  units were harvested and filtered through an 0.8- $\mu$ m nylon membrane and prewashed with 3 ml water, followed by another 3-ml water wash after cell filtration. The membranes were placed in 1.5 ml extraction solution (0.1 M formic acid, 15.3 M acetonitrile), flash-frozen in liquid nitrogen, and stored at  $-80^\circ C$ . Before analysis, the extracts were vortexed for 15 min and centrifuged to collect the supernatants at 4°C. Glucose 6-phosphate and fructose 1,6-bisphosphate were separated and identified using a 1200 Series liquid chromatography instrument (Agilent Technologies, Santa Clara, CA). One microliter of each sample was injected onto an Agilent Eclipse XDB-C<sub>18</sub> (2.1-mm inside diameter [i.d.], 150-mm length, 3.5- $\mu$ m particle size) column with a Zorbax SB-C<sub>8</sub> (2.1-mm i.d., 12.5-mm length, 5- $\mu$ m particle size) guard column and eluted at 25°C and a flow rate of 0.2 ml/min with the following gradient (modification from reference 41): 15 min isocratic 100% buffer A (10 mM tributylamine-15 mM acetic acid), then in 15 min with a linear gradient to 60% buffer B (methanol), 2 min isocratic 60% B, and then a 10-min equilibration with 100% buffer A. The eluent from the column was introduced into a mass spectrometer for 25 min after the first 10 min. Mass spectrometry (MS) was performed on an LTQ XL ion trap instrument (Thermo Fisher Scientific, San Jose, CA) with an electrospray ionization (ESI) source operated in negative ion mode. The MS settings were capillary temperature of 350°C, ion spray voltage of 4.5 kV, sheath gas flow of 60

(arbitrary units), auxiliary gas flow of 10 (arbitrary units), and sweep gas flow of 5 (arbitrary units). For the MS/MS product ion scan, the scan range was  $m/z$  80 to  $m/z$  300. The compounds G6P at  $m/z$  259.1 and F1,6BP at  $m/z$  339.1 were isolated with an  $m/z$  2 isolation width and fragmented with a normalized collision-induced dissociation energy setting of 35% and with an activation time of 30 ms and an activation  $Q$  of 0.250.

The significance threshold between cells provided with cellobiose and cells provided with glucose was set at a  $P$  value of 0.01. Five biological replicates were used in each sample group. Only the metabolites with higher than a 2-fold change between each sample group were included in the analysis.

**Plasma membrane isolation.** Strains were subjected to cellobiose fermentation under anaerobic conditions. Yeast cells with an  $OD_{600}$  equivalent to 40 were harvested at mid-log phase and flash-frozen in liquid nitrogen. Membrane fractions were extracted based on the protocol published in reference 42.

**Pma1 ATPase activity assay.** The ATPase assay described in reference 26 was modified as follows. Thirty micrograms of the isolated membrane fraction was incubated in assay buffer (50 mM 2-(*N*-morpholino)ethanesulfonic acid [MES], pH 5.7, 10 mM  $MgSO_4$ , 50 mM KCl, 5 mM  $NaN_3$ , 50 mM  $KNO_3$ ) with and without 3 mM orthovanadate for 25 min at 30°C. A 1.8 mM concentration of ATP was added to start the reactions in the 100- $\mu$ l reaction mixtures. The reaction mixtures were incubated at 30°C for 15 min, and then the membranes were isolated from the reaction mixtures by centrifugation at  $13,000 \times g$  for 10 min at 4°C. The released inorganic phosphate was measured in the supernatant using the ATPase/GTPase activity assay kit (Sigma-Aldrich) based on the manufacturer's protocol. The specific Pma1 ATPase activities were calculated by subtracting the concentration of released inorganic phosphate in reaction mixtures provided with orthovanadate from the concentration in those without orthovanadate.

**Yeast cell-based cellobiose uptake assay.** The cell-based cellobiose uptake assay was modified from reference 43. Yeast strains were grown to mid-exponential phase in 2% oMM glucose, washed with assay buffer (5 mM MES, 100 mM NaCl, pH 6.0) three times, and resuspended to a final  $OD_{600}$  of 10. Equal volumes of the cell suspension and 200  $\mu$ M cellobiose were mixed to start the reactions, and the reaction mixtures were incubated at 30°C with continuous shaking for 15 min. The reactions were stopped by adding 150  $\mu$ l of supernatants to 150  $\mu$ l 0.1 M NaOH. The concentrations of the remaining cellobiose were measured using an ICS-3000 ion chromatography system (Dionex, Sunnyvale, CA, USA) equipped with a CarboPac PA200 carbohydrate column. The column was eluted with a sodium acetate (NaOAc) gradient in 100 mM NaOH at a flow rate of 0.4 ml/min and at 30°C.

## SUPPLEMENTAL MATERIAL

Supplemental material for this article may be found at <https://doi.org/10.1128/mBio.00855-17>.

**FIG S1**, TIF file, 7.2 MB.

**FIG S2**, TIF file, 2.3 MB.

**FIG S3**, TIF file, 2.7 MB.

**TABLE S1**, XLSX file, 0.01 MB.

## ACKNOWLEDGMENTS

We thank Raissa Estrela, Xin Li, Ligia Acosta-Sampson, Yuping Lin, and Matt Shurtleff for helpful discussions and contributions.

This work was supported by funding from the Energy Biosciences Institute to J.H.D.C. and from the National Institutes of Health (R01CA172667) to D.K.N. Publication made possible in part by support from the Berkeley Research Impact Initiative (BRII) sponsored by the UC Berkeley Library.

All authors contributed to the design of the experiments. K.C. and D.I.B. carried out the experiments. D.K.N. and J.H.D.C. aided in interpretation of the systems-level experiments. K.C. wrote the manuscript, with editing by D.I.B., D.K.N., and J.D.H.C.

## REFERENCES

- van Heerden JH, Wortel MT, Bruggeman FJ, Heijnen JJ, Bollen YJM, Planqué R, Hulshof J, O'Toole TG, Wahl SA, Teusink B. 2014. Lost in transition: start-up of glycolysis yields subpopulations of nongrowing cells. *Science* 343:1245-1248. <https://doi.org/10.1126/science.1245114>.
- Youk H, van Oudenaarden A. 2009. Growth landscape formed by perception and import of glucose in yeast. *Nature* 462:875-879. <https://doi.org/10.1038/nature08653>.
- Ha SJ, Galazka JM, Kim SR, Choi JH, Yang X, Seo JH, Glass NL, Cate JHD, Jin YS. 2011. Engineered *Saccharomyces cerevisiae* capable of simultaneous cellobiose and xylose fermentation. *Proc Natl Acad Sci U S A* 108:504-509. <https://doi.org/10.1073/pnas.1010456108>.
- Galazka JM, Tian C, Beeson WT, Martinez B, Glass NL, Cate JHD. 2010. Cellodextrin transport in yeast for improved biofuel production. *Science* 330:84-86. <https://doi.org/10.1126/science.1192838>.
- Lin Y, Chomvong K, Acosta-Sampson L, Estrela R, Galazka JM, Kim SR, Jin YS, Cate JH. 2014. Leveraging transcription factors to speed cellobiose fermentation by *Saccharomyces cerevisiae*. *Biotechnol Biofuels* 7:126. <https://doi.org/10.1186/s13068-014-0126-6>.
- Daran-Lapujade P, Rossell S, van Gulik WM, Luttk MAH, de Groot MJL, Slijper M, Heck AJ, Daran JM, de Winder JH, Westerhoff HV, Pronk JT, Bakker BM. 2007. The fluxes through glycolytic enzymes in *Saccharomyces cerevisiae* are predominantly regulated at posttranscriptional levels. *Proc Natl Acad Sci U S A* 104:15753-15758. <https://doi.org/10.1073/pnas.0707476104>.
- Kim H, Lee WH, Galazka JM, Cate JHD, Jin YS. 2014. Analysis of cellodextrin transporters from *Neurospora crassa* in *Saccharomyces cerevisiae* for cellobiose fermentation. *Appl Microbiol Biotechnol* 98:1087-1094. <https://doi.org/10.1007/s00253-013-5339-2>.

8. Bañuelos M, Gancedo C, Gancedo JM. 1977. Activation by phosphate of yeast phosphofructokinase. *J Biol Chem* 252:6394–6398.
9. Avigad G. 1981. Stimulation of yeast phosphofructokinase activity by fructose 2,6-bisphosphate. *Biochem Biophys Res Commun* 102:985–991. [https://doi.org/10.1016/0006-291X\(81\)91635-1](https://doi.org/10.1016/0006-291X(81)91635-1).
10. Nissler K, Otto A, Schellenberger W, Hofmann E. 1983. Similarity of activation of yeast phosphofructokinase by AMP and fructose-2,6-bisphosphate. *Biochem Biophys Res Commun* 111:294–300. [https://doi.org/10.1016/S0006-291X\(83\)80150-8](https://doi.org/10.1016/S0006-291X(83)80150-8).
11. Rodicio R, Strauss A, Heinisch JJ. 2000. Single point mutations in either gene encoding the subunits of the heterooctameric yeast phosphofructokinase abolish allosteric inhibition by ATP. *J Biol Chem* 275:40952–40960. <https://doi.org/10.1074/jbc.M007131200>.
12. Gradmann D, Hansen UP, Long WS, Slayman CL, Warncke J. 1978. Current-voltage relationships for the plasma membrane and its principal electrogenic pump in *Neurospora crassa*: I. Steady-state conditions. *J Membr Biol* 39:333–367. <https://doi.org/10.1007/BF01869898>.
13. Serrano R. 1983. In vivo glucose activation of the yeast plasma membrane ATPase. *FEBS Lett* 156:11–14. [https://doi.org/10.1016/0014-5793\(83\)80237-3](https://doi.org/10.1016/0014-5793(83)80237-3).
14. Mason AB, Allen KE, Slayman CW. 2014. C-terminal truncations of the *Saccharomyces cerevisiae* PMA1 H<sup>+</sup>-ATPase have major impacts on protein conformation, trafficking, quality control, and function. *Eukaryot Cell* 13:43–52. <https://doi.org/10.1128/EC.00201-13>.
15. Rao R, Drummond-Barbosa D, Slayman CW. 1993. Transcriptional regulation by glucose of the yeast PMA1 gene encoding the plasma membrane H<sup>(+)</sup>-ATPase. *Yeast* 9:1075–1084. <https://doi.org/10.1002/yea.320091006>.
16. García-Arranz M, Maldonado AM, Mazón MJ, Portillo F. 1994. Transcriptional control of yeast plasma membrane H<sup>(+)</sup>-ATPase by glucose. Cloning and characterization of a new gene involved in this regulation. *J Biol Chem* 269:18076–18082.
17. Kang WK, Kim YH, Kang HA, Kwon KS, Kim JY. 2015. Sir2 phosphorylation through cAMP-PKA and CK2 signaling inhibits the lifespan extension activity of Sir2 in yeast. *Elife* 4:e09709. <https://doi.org/10.7554/eLife.09709>.
18. Eraso P, Mazón MJ, Portillo F. 2006. Yeast protein kinase Ptk2 localizes at the plasma membrane and phosphorylates in vitro the C-terminal peptide of the H<sup>+</sup>-ATPase. *Biochim Biophys Acta* 1758:164–170. <https://doi.org/10.1016/j.bbame.2006.01.010>.
19. Portillo F, Eraso P, Serrano R. 1991. Analysis of the regulatory domain of yeast plasma membrane H<sup>+</sup>-ATPase by directed mutagenesis and intragenic suppression. *FEBS Lett* 287:71–74. [https://doi.org/10.1016/0014-5793\(91\)80018-X](https://doi.org/10.1016/0014-5793(91)80018-X).
20. Lecchi S, Nelson CJ, Allen KE, Swaney DL, Thompson KL, Coon JJ, Sussman MR, Slayman CW. 2007. Tandem phosphorylation of Ser-911 and Thr-912 at the C terminus of yeast plasma membrane H<sup>+</sup>-ATPase leads to glucose-dependent activation. *J Biol Chem* 282:35471–35481. <https://doi.org/10.1074/jbc.M706094200>.
21. Eraso P, Portillo F. 1994. Molecular mechanism of regulation of yeast plasma membrane H<sup>(+)</sup>-ATPase by glucose. Interaction between domains and identification of new regulatory sites. *J Biol Chem* 269:10393–10399.
22. Goossens A, de La Fuente N, Forment J, Serrano R, Portillo F. 2000. Regulation of yeast H<sup>(+)</sup>-ATPase by protein kinases belonging to a family dedicated to activation of plasma membrane transporters. *Mol Cell Biol* 20:7654–7661. <https://doi.org/10.1128/MCB.20.20.7654-7661.2000>.
23. Rolland F, Winderickx J, Thevelein JM. 2002. Glucose-sensing and -signalling mechanisms in yeast. *FEMS Yeast Res* 2:183–201.
24. Ozcan S, Dover J, Rosenwald AG, Wölfel S, Johnston M. 1996. Two glucose transporters in *Saccharomyces cerevisiae* are glucose sensors that generate a signal for induction of gene expression. *Proc Natl Acad Sci U S A* 93:12428–12432. <https://doi.org/10.1073/pnas.93.22.12428>.
25. Xue Y, Battle M, Hirsch JP. 1998. GPR1 encodes a putative G protein-coupled receptor that associates with the Gpa2p Galpha subunit and functions in a Ras-independent pathway. *EMBO J* 17:1996–2007. <https://doi.org/10.1093/emboj/17.7.1996>.
26. Viegas CA, Sá-Correia I. 1991. Activation of plasma membrane ATPase of *Saccharomyces cerevisiae* by octanoic acid. *J Gen Microbiol* 137:645–651. <https://doi.org/10.1099/00221287-137-3-645>.
27. Pontes MH, Sevostyanova A, Groisman EA. 2015. When too much ATP is bad for protein synthesis. *J Mol Biol* 427:2586–2594. <https://doi.org/10.1016/j.jmb.2015.06.021>.
28. Browne SE. 2013. When too much ATP is a bad thing: a pivotal role for P2X7 receptors in motor neuron degeneration. *J Neurochem* 126:301–304. <https://doi.org/10.1111/jnc.12321>.
29. Larsson C, Nilsson A, Blomberg A, Gustafsson L. 1997. Glycolytic flux is conditionally correlated with ATP concentration in *Saccharomyces cerevisiae*: a chemostat study under carbon- or nitrogen-limiting conditions. *J Bacteriol* 179:7243–7250. <https://doi.org/10.1128/jb.179.23.7243-7250.1997>.
30. Mazón MJ, Eraso P, Portillo F. 2015. Specific phospho-antibodies reveal two phosphorylation sites in yeast Pma1 in response to glucose. *FEMS Yeast Res* 15:fov030. <https://doi.org/10.1093/femsyr/fov030>.
31. Thomsson E, Larsson C, Albers E, Nilsson A, Franzén CJ, Gustafsson L. 2003. Carbon starvation can induce energy deprivation and loss of fermentative capacity in *Saccharomyces cerevisiae*. *Appl Environ Microbiol* 69:3251–3257. <https://doi.org/10.1128/AEM.69.6.3251-3257.2003>.
32. Dechant R, Peter M. 2014. Cytosolic pH: a conserved regulator of cell growth? *Mol Cell Oncol* 1:e969643. <https://doi.org/10.4161/23723548.2014.969643>.
33. Thevelein JM, Hohmann S. 1995. Trehalose synthase: guard to the gate of glycolysis in yeast? *Trends Biochem Sci* 20:3–10. [https://doi.org/10.1016/S0968-0004\(00\)88938-0](https://doi.org/10.1016/S0968-0004(00)88938-0).
34. Choi KM, Kwon YY, Lee CK. 2015. Disruption of Snf3/Rgt2 glucose sensors decreases lifespan and caloric restriction effectiveness through Mth1/Std1 by adjusting mitochondrial efficiency in yeast. *FEBS Lett* 589:349–357. <https://doi.org/10.1016/j.febslet.2014.12.020>.
35. Moriya H, Johnston M. 2004. Glucose sensing and signaling in *Saccharomyces cerevisiae* through the Rgt2 glucose sensor and casein kinase I. *Proc Natl Acad Sci U S A* 101:1572–1577. <https://doi.org/10.1073/pnas.0305901101>.
36. Flick KM, Spielwog N, Kalashnikova TI, Guaderrama M, Zhu Q, Chang HC, Wittenberg C. 2003. Grr1-dependent inactivation of Mth1 mediates glucose-induced dissociation of Rgt1 from HXT gene promoters. *Mol Biol Cell* 14:3230–3241. <https://doi.org/10.1091/mbc.E03-03-0135>.
37. Lakshmanan J, Mosley AL, Ozcan S. 2003. Repression of transcription by Rgt1 in the absence of glucose requires Std1 and Mth1. *Curr Genet* 44:19–25. <https://doi.org/10.1007/s00294-003-0423-2>.
38. Jouandot D, Roy A, Kim JH. 2011. Functional dissection of the glucose signaling pathways that regulate the yeast glucose transporter gene (HXT) repressor Rgt1. *J Cell Biochem* 112:3268–3275. <https://doi.org/10.1002/jcb.23253>.
39. Ryan OW, Skerker JM, Maurer MJ, Li X, Tsai JC, Poddar S, Lee ME, DeLoache W, Dueber JE, Arkin AP, Cate JHD. 2014. Selection of chromosomal DNA libraries using a multiplex CRISPR system. *Elife* 3:e03703. <https://doi.org/10.7554/eLife.03703>.
40. Benjamin DJ, Louie SM, Mulvihill MM, Kohnz RA, Li DS, Chan LG, Sorrentino A, Bandyopadhyay S, Cozzo A, Ohiri A, Goga A, Ng SW, Nomura DK. 2014. Inositol phosphate recycling regulates glycolytic and lipid metabolism that drives cancer aggressiveness. *ACS Chem Biol* 9:1340–1350. <https://doi.org/10.1021/cb5001907>.
41. Luo B, Groenke K, Takors R, Wandrey C, Oldiges M. 2007. Simultaneous determination of multiple intracellular metabolites in glycolysis, pentose phosphate pathway and tricarboxylic acid cycle by liquid chromatography-mass spectrometry. *J Chromatogr A* 1147:153–164. <https://doi.org/10.1016/j.chroma.2007.02.034>.
42. Kaiser CA, Chen EJ, Losko S. 2002. Subcellular fractionation of secretory organelles. *Methods Enzymol* 351:325–338. [https://doi.org/10.1016/S0076-6879\(02\)51855-3](https://doi.org/10.1016/S0076-6879(02)51855-3).
43. Li X, Yu VY, Lin Y, Chomvong K, Estrela R, Park A, Liang JM, Znameroski EA, Feehan J, Kim SR, Jin YS, Glass NL, Cate JHD. 2015. Expanding xylose metabolism in yeast for plant cell wall conversion to biofuels. *Elife* 4:e05896. <https://doi.org/10.7554/eLife.05896>.